Microbead models in glaucoma

James E Morgan[a]
James R Tribble[a]

[a] School of Optometry and Vision Sciences
Cardiff University
Maindy Road
Cardiff University CF24 4LU
Cardiff, United Kingdom
Tel: 00442920874374

Pages 19
Figures 2
Tables1

Corresponding author

James E Morgan
School of Optometry and Vision Sciences
Cardiff University
Maindy Road
Cardiff University CF24 4LU
Cardiff, United Kingdom
Tel: 00442920874374

Morganje3@cardiff.ac.uk

Keywords

Glaucoma, Microbead, Animal Model, Rodent, Primate

Commercial interest: None.

Abstract

The sustained and moderate elevation of intraocular pressure, which can be initiated at precise time points, remains the cornerstone of research into the mechanisms of glaucomatous retinal damage. We focus on the use of microbeads to block the outflow of aqueous following anterior chamber injection in a range of animals (mouse, rat and primate). We describe some of the most commonly used parameters and present guidance on injection technique and bead manipulation to maximize the successful generation of experimental glaucoma.

1.0 Introduction

The study of glaucomatous pathophysiology has relied on the development of technologies to generate sustained and moderate increases in intraocular pressure in a range of species. The chronic elevation of intraocular pressure (IOP) presents significant challenges in small eyes where ocular tissues are thin and vulnerable to the effects of inflammation and remodeling.

The choice of animal is guided by cost, handling characteristics and the availability of mutant strains. Not surprisingly, rodents have superseded primates as the most common experimental model for the investigation of mechanism underlying retinal ganglion cell loss. For the rat, the injection of hypertonic saline for the sclerosis of episcleral vessels has been one of the most successful models (Morrison *et al.*, 2008) but its use has been constrained by need for a high level of surgical skill to cannulate small episcleral veins. With the mouse, genetic models of glaucoma such as the DBA2J strain which rely on the deposition of pigment cells within the trabecular meshwork (TM) (John *et al.*, 1998) have the advantage that they do not require surgical intervention for the development of ocular hypertension. However, the model incurs significant financial and time costs since animals have to be aged before glaucoma develops and control of IOP at the single animal level can be problematic (John, 2005). Other models in which the episcleral vessels are cauterized externally raise the possibility of the confounding effects of increases in episcleral venous pressure (Vecino and Sharma, 2011).

A cost effective model would be one in which the induction of IOP elevation is technically undemanding, rapid in onset and works in as many animals as possible. In the last decade the availability of high quality microbeads with diameters that match the pores in the TM has facilitated the generation of sustained ocular hypertension in primates and rodents. With these methods, the onset of ocular hypertension can be timed and the level of the IOP increase controlled. In this review we cover the salient features of currently used models with technical advice on methods of bead delivery.

2.0 Background

Obstruction of the TM by the injection of microparticles has a long track record as a method for the generation of experimental glaucoma. Some of the earliest attempts were based on primate models in which glutaraldehyde treated autologous red blood cells were injected into the anterior chamber. These cells mimicked the ghost red blood cells (GBCs) in their occlusion of the TM by virtue of their membrane rigidity. Sustained elevation in IOP could be achieved in both rabbit and primates (Squirrel and Cynomolgous monkeys) (Quigley and Addicks, 1980) and electron microscopy revealed considerable numbers of deformed GBCs trapped within the TM. While the injection technique was straightforward, it was limited in that peak IOP increase could be difficult to control and tended to be high (mean IOP in primates of 53.5 mmHg, mean peak of 69.8 mmHg). At these IOP levels corneal edema was a common feature which could confound the accurate measurement of IOP because of the increases in corneal thickness. The mean and peak values were lower for the rabbit eyes but corneal ectasia was a significant side effect. Furthermore, for a sustained increase in IOP almost 75% of the anterior chamber had to be filled with red blood cells which could compromise fundoscopy. While this model resulted in retinal ganglion cell loss, it had greater relevance for the study of retinal ganglion cell death in acute, rather than chronic, glaucoma.

In light of these considerations, subsequent primate glaucoma models relied on laser treatment of the TM. The appeal of this approach was that it resulted in moderate increases in IOP which could be titrated and the laser treatment repeated to achieved the desired increase in IOP (Gaasterland and Kupfer, 1974). The method has been used for many of the key studies outlining early pathological damage in glaucoma (Quigley, 1999) and remains in use for structural analysis of changes in the lamina cribrosa (Burgoyne *et al.*, 2005). Furthermore, the technique can be used in rabbits to induce robust increases in IOP 9 (Gherezghiher *et al.*, 1986), though the problem of corneal ectasia with substantial IOP increases remains. Since these models require

dedicated laser facilities, they remain the preserve of a small number of suitably equipped laboratories.

The primate remains an excellent model for mapping structural and morphological changes within the retina and optic nerve head. However, it has significant drawbacks with regard to mechanistic studies of glaucoma pathology. In this respect, rodents present a more tractable model in terms of the ability to create genetic constructs or to undertake cost effective studies of retinal and optic nerve changes in glaucoma. Mice can be bred and manipulated to enhance or delete the activity of relevant genes – a facility which is increasingly available through gene editing techniques for the rat (Sander and Joung, 2014).

In the 1980s the role of microparticle occlusion of the TM was revisited, with the development of microbeads for use in cell and molecular biology. The beads were available in sizes that matched the pores in the TM and the demonstration that these could be incorporated in the TM by phagocytosis recommended their use for the obstruction of aqueous outflow (Matsumoto and Johnson, 1997). For the primate, microbead injections were first used by Weber and Zelenak for the induction of experimental glaucoma (Weber and Zelenak, 2001). The model generated effective and sustained increases in IOP but this required repeat injections (on a weekly basis in many animals) since the beads fell within the anterior chamber under the influence of gravity. Importantly, IOP increases were seen following partial fills of the anterior chamber thereby maintaining a clear visual axis for fundus imaging. The downside of this model is that it generates IOP spikes which could complicate the correlation of IOP elevation with retinal ganglion cell damage; clinical studies have suggested that spiking IOPs are an independent variable in the progression of glaucoma damage (Asrani *et al.*, 2000). An important technical consideration was that the microbeads had to be thoroughly washed prior to injection to prevent preservative agents in the bead carrier solutions from causing anterior chamber inflammation (Weber pers. communication). Sterilisation of the beads by gamma irradiation was used to guard against endophthalmitis.

3.0 Mouse

The small anterior chamber of the rodent eye is ideal for microbead occlusion. The mouse has particular appeal because of the availability of numerous genetic constructs and the ability to measure IOP in awake (manually or by telemetry (Ruixia, 2008)) and anaesthetized animals (Wang *et al.*, 2005; Cone *et al.*, 2012).

The use of microbeads in mouse glaucoma models has generated a wide range of injection parameters and techniques which are summarized in table 1. The table is not intended as an exhaustive list of microbead glaucoma models but to illustrate the range of injection parameters and IOP elevation. Direct comparison between models is difficult because of the lack of standardized outcomes but there is a broad consensus that the intraocular pressure can be elevated in the mouse eye following one or more anterior chamber injections with microbreads. To date, the maximum number of beads injected (Frankfort *et al.*, 2013) is as a mixture of $4.7x10^6$ (6µm) and $2.4x10^7$ (1µm) in 1-2µL (total volume) to generate a mean increase of 15.3(5.6) mmHg over a 12 week period following a single injection. By contrast, Sappington, used bead numbers 3-4 orders of magnitude lower at 10^3 beads to produce a higher mean IOP of 20.0(0.8) after 2 injections with injection volumes ranging from 1-3µl. Cone et al. provided an informative analysis of the effect of mixing beads of different sizes on the development of IOP elevation with their '4+1' mixture of beads ($3x10^6$,6µm + $1.5 x10^7$,1µm) delivering the greatest optic nerve damage when measured over a 28 week interval. The choice of bead size is an important practical consideration; larger beads are easier to view and manipulate but they carry a greater risk of occluding the injection cannula. Surprisingly, there does not appear to be a clear relationship between the total volume of beads injected and the increase in IOP (Figure 2). Satisfactory increases in IOP with similar levels of retinal ganglion cell loss were reported in all animals which may reflect the efficiency of using fewer, larger beads. Further work with standardized outcome measures would greatly help in the selection of the optimum injection parameters.

Consideration of the volume of the anterior chamber of the mouse eye is instructive when considering the optimal injection volume. Functional

estimations of the anterior chamber volume for the mouse eye indicate that this is approximately 7µl (Zhang *et al.*, 2002). The geometric estimate of anterior chamber volume is lower; histological measurements, taking into account corneal thickness, corneal curvature and anterior lens curvature give the volume of the mouse anterior chamber of 3.94µl (Remtulla and Hallett, 1985). Cone and Frankfort et al. followed up the bead injections with 3µL of viscoelastic which would therefore occupy c. 50-80% of the anterior chamber and contribute to an increase in IOP independent of any bead occlusion by virtue of its space occupying properties. What is striking is that in the mouse eye a 3% increase in anterior chamber volume (7 to 7.2µl) can generate a doubling in IOP from 15 to 30mm Hg (Zhang *et al.*, 2002). The extent to which the viscosity of the viscoelastic agent alters the stiffness of the cornea has not been measured but is a topic worth further investigation since it could estimate the accuracy of IOP in these models.

4.0 Rat

There are advantages to working on rat, rather than mouse glaucoma models. Rat eyes are larger and therefore easier to inject and rats can be easier to handle in the context of obtaining awake IOP readings. The rat is increasingly being used for mechanistic studies of glaucoma pathophysiolgy, supported by the increasing availability of genetically altered rats (Ma *et al.*, 2014). Gene array analyses in wild type strains have been valuable in pinpointing potential mechanism for early axonal damage (Johnson *et al.*, 2011; Agudo et al., 2008).

Urcola et al. (2006) has provided the most comprehensive review of microbead injection protocols in the rat. They compared anterior segment injections in Sprague Dawley rats with 10µm latex spheres (table 1) with and without the addition of a viscoelastic agent (hydroxypropylmethylcellulose, HPM). The maintenance of IOP elevation required multiple anterior segment injections (9 injections over 30 weeks) but fewer injections in those eyes receiving HPM. In both sets of eyes with microbead injections, there was a tendency for the IOP to increase slowly over time so that the peak IOPs were seen at 30 weeks in eyes with HPM injections and at 24 weeks in those eyes with beads alone. The level of IOP increase was slightly higher in the HPM

injected eyes. The volume of injected agent in both cases was 20µL which is a greater proportion of the anterior segment volume for the rat eye compared with injections volumes used in the mouse eye (Remtulla and Hallett, 1985). The location of the beads is not recorded in this paper- but rats underwent fundoscopy prior to sacrifice suggesting that, at least by 30 weeks, the visual axis was relatively clear.

With all bead models, the maintenance of optical clarity is important for monitoring retinal health and for the physiological assessment of retinal function. No bead models have been used for invasive electrophysiological assessment of retinal ganglion cells and the only published study is based on an episcleral cautery model (King *et al.*, 2006). It is likely that the majority of microbead models result in some obscuration of the visual axis. To minimise this effect, Samsel et al. developed a method in which magnetic microspheres were injected into the anterior chamber and then relocated to reside within the anterior segment thereby minimizing the location of beads over the pupil (Samsel *et al.*, 2011). The beads are sterilized by gamma irradiation prior to use and result in minimal anterior segment inflammation. Just prior to injection they are re-suspended in solution (BSS, Alcon) and then injected using a 32-33 Gauge needle. A Neodymium Boron (NdB, rare earth) magnet (strength c.0.45T) is quite sufficient to relocate the beads. The magnetic flux can be shaped to a fine point using a machined soft iron core which can be attached to the tip of the magnet to allow for precise location of the beads throughout the anterior segment.

The model has subsequently been used by others to deliver robust and prolonged elevations in IOP lasting 2-4 weeks following a single injection (Foxton *et al.*, 2013; Dai *et al.*, 2012). A novel refinement has been to place a cylindrical magnet (with the magnetic poles at 90 degrees to the axis of the cylinder) over the anterior chamber to allow for the rapid transfer of beads to the iridocorneal angle (Bunker *et al.*, 2015).

5.0 Variables affecting IOP increase

5.1 Cannulation technique

Rodents have thin corneas which present a particular challenge for the retention of beads. These incisions are more challenging with the rodent eyes where the corneal thickness is in the range 160 µm for the rat eye to 90 µm for the mouse eye (Bawa *et al.*, 2013). In the mouse, the use of a glass injection micropipette is optimal since these can be pulled to very fine outside diameters and bevelled to a sharp tip. For 10µm beads, a cannula with an external diameter of 100um should facilitate bead retention in the anterior chamber and minimise cannula blockage. In some models, the injection site is prepared with incision using a larger needle which may compromise bead retention. For example Frankfort et al. (2013) made an initial corneal hole with a 30G needle which has an external diameter of 300µm (approximately 10% of the corneal diameter) followed by the insertion of a 75µm (outside diameter) cannula. These difficulties can be mitigated if the injection track is made tangential to the corneal surface (Urcola *et al.*, 2006) to create a self sealing incision, a technique that is routinely used in modern cataract surgery (Fine, 1991). In humans, where the corneal stromal thickness is of the order of 500µm, a self sealing incision can be constructed simply by traversing the corneal thickness. For a 34 guage needle the outside diameter is 190µm indicating that the needle can only partially track within the thickness of the corneal stroma. The use of tribevelled needles (NanoFil needle, Item#: NF34BV-2, World Precision Instruments) can facilitate clean anterior chamber injections and these needles can be re-sharpened using a microbeveller.

With the magnetic bead model, the microbeads can be dissociated from the delivery of the carrier solution by gentle angulation of the needle within the tunneled incision to facilitate egress of aqueous and carrier solution during the injection. Since the beads are drawn away from the injections site during this process- microbead loss is minimized. Furthermore, the microbeads can be trapped within the iridocorneal angle if the anterior chamber is shallowed once the injection has been completed.

5.2 Injection time

The level of IOP elevation can be shaped by the time course of the bead injections. Since this is not systematically recorded for the various models comparison between publications can be difficult. The effect of acute IOP elevation was explored by Smedwoski et al. (2014) in the rat in which the injection volume of 15µl was injected rapidly over a 5 second period; the cornea was noted to be edematous as a result which took approximately 6 hours to resolve. Optic nerve damage was determined on the basis of axon counts and on average was reduced to 30% of control after 6-weeks. The IOP increase was estimated at over 55 mmHg for the first port injection day, falling to 24mmHg after 6 weeks. The authors used a viscoelastic agent (Microvisc) to seal the injection site and reported improved occlusion with a mixture of beads (4+1 model) in which 2µl of 6 µm beads was followed by 2µl of 1µm beads and then 1ul of Healon. Importantly this protocol generated moderate increase in IOP (mean 6.1) but with a mean IOP of 36 mm Hg- typically seen at the 7-day period.

5.3 Species differences

For the rat, the degree of RGC loss over a 4-6 week period is typically 20-30% for Brown Norway and Sprague Dawley strains. It is interesting to note the high level of damaged noted by Dai et al. (2012) using Albino Swiss rats.

In the mouse the relationship between strain, IOP elevation and cell loss is complicated. The relationship was explored by Cone et al who compared the effects of microbead IOP elevation on CD1, DBA/2J and C57/B6 young and old mice. They found that the greatest damage to the RGC layer occurred in the CD1 (10 months) and young C57/BL6 (2 months) animals with relatively little change in the older C57/BL6 (8 months). The lack of damage in the elderly eyes is interesting and counterintuitive since the physiologic resilience of retinal ganglion cells is likely to reduce with age (Baltan *et al.*, 2010).

6.0 Conclusion

Microbead injection models are in routine use for the development of experimental glaucoma in rodents and primates. They allow the generation of persistent ocular hypertension and some element of control for the level of IOP elevation. The use of fluorescent markers can greatly facilitate the identification of beads within the anterior chamber while the use of ferromagnetic particles allows the injection of beads and carrier solution to be separated and for a clear visual axis to be maintained. The adjunctive use of viscoelastic agents can be useful to position beads within the iridocorneal angle; caution should be exercised in their use until more is known of their effect on corneal rigidity and, by extension on the accuracy of IOP readings.

Table 1

Summary of commonly used microbead models for primate, rat and mouse models of glaucoma.

Author	Species	vol	Viscoelastic	Bead type	Bead size	[Bead]	IOP max (SD) (mmHg)	IOP mean (SD) (mmHg)	Damage (SD)	Duration	Comment
Weber & Zelenak (2001)	Primate (macaque)	50-100uL	NA	Latex microspheres	10 um	2-4x10^5	50.9(17.5)	26.7(7.5)	70% decrease in axon count	30-144 weeks	3-12 injections per animal
Cone et al. (2012)	Mouse	'3+2'	2uL visco	Polystyrene	1.5uL 6um + 1.5uL 1um	3x10^6 6um + 1.5 x10^7 1um	NA	12.9(2.8)	15(24)	28 weeks	C57BL/6
Cone et al. (2012)	Mouse	'4+1'	1ul visco	Polystyrene	2uL 6um + 2uL 1um	3x10^6 6um + 1.5 x10^7 1um	NA	18.6(5.1)	36(34)	28 weeks	C57BL/6
Cone et al. (2012)	Mouse	'2+3'	3uL	Polystyrene	6um	3x10^6 6um + 1.5 x10^7 1um	NA	12.5(3.1)	15(24)	28 weeks	C57BL/6
Frankfort et al. (2013)	Mouse C57BL/6	1-2uL	3uL Provisc	Polystyrene	1um + 6um	4.7x10^6 6um + 2.4 x10^7 1um	NA	15.3(5.6)	11.2 (NA)	12 weeks	C57BL/6 Single injection1
Sappington et al. (2010)	Mouse C57BL/6	1uL	NA	Polystyrene (fluorescent)	15um	1x10^3	NA	20.0(0.8)	27%(NA) ON counts	2-4 weeks	100um pipette
Sappington et al (2010)	Rat (BN)	2-7uL	NA	Polystyrene (fluorescent)	15um	2.5-7.0x10^3	NA	29.7(1.2) 7uL 28.8 (1.6) 5uL 26.9 (1.7) 2 uL	16% (NA) ON counts(5uL)	Up to 8 weeks	2nd injection at 2 weeks
Urcola et al. (2006)	Rat (SD, albino)	20uL	NA	Latex microspheres	10 um	2-4x10^5	37.6(2.6)	28.1 (0.7)	23.1(2)% RGC counts	30 weeks	30 Gauge needle: tangential method: weekly
Urcola et al. (2006)	Rat (SD, Albino)	10uL	10uL hydroxypropylemthylcellulose	Latex microspheres	10 um	1-2x10^5	42.5(1.7)	31.1(0.6)	27.2(2.1)% RGC counts	30 weeks	30 Gauge needle: tangential method: weekly

Samsel et al. (2011)	Rat (BN)	10-20uL	NA	Polystyrene Ferromagnetic	5um	4.7x10^5*	54(NA)	29.4(0.9)	36.4(2.4) RGC layer counts	6 weeks	32-33 Gauge needle 2 pole magnet
Dai et al. (2012)	Rat (Albino Swiss)	20uL	NA	Polystyrene Ferromagnetic (Aldehyde terminated)	5um	NA	43(2.3)	36.7	81% ON counts	4 weeks	33 Gauge needle, 2 pole magnet
Foxton et al. (2013)	Rat (BN)	25uL	NA	Polystyrene Ferromagnetic	8um	NA	55.2(3.5)	43.3(3.3)	x20 increase in degenerating axons	17 days	NA Ring magnet
Smedowski et al. (2014)	Rat (Wistar)	'10+5'	5uL visco	Polystyrene	5uL 10um + 5uL 6um	NA	NA	30.9(3.2)	28% ON counts	6 weeks	22 Gauge needle with 50um glass microneedle

*count performed on new bead preparation (4.5 um, Kisker Biotech)

Figures

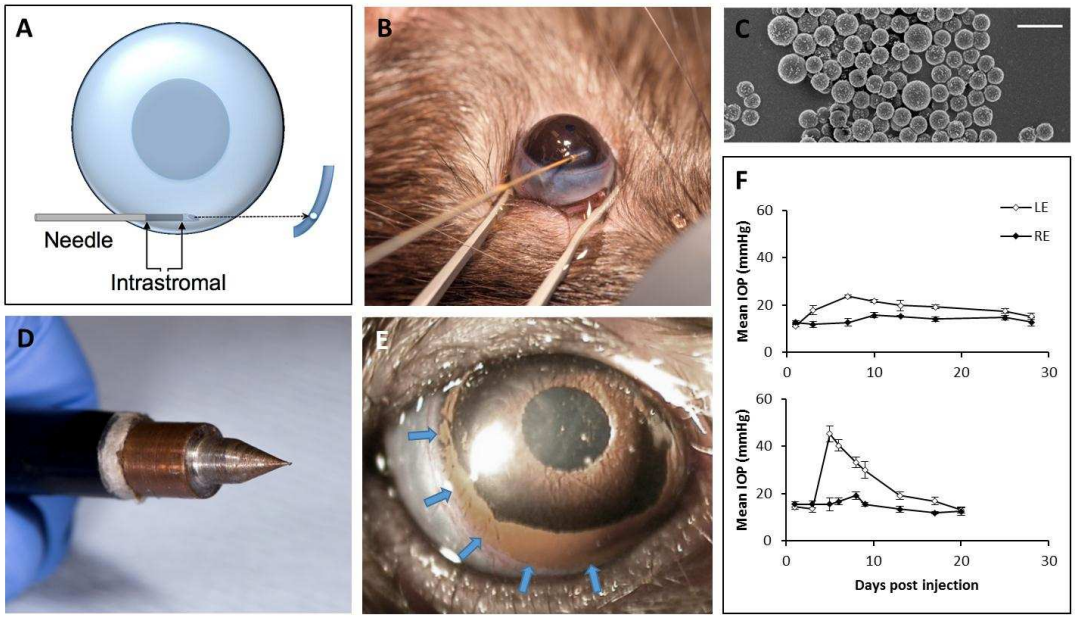

Figure1. A) Diagram and B) image showing injection method; intrastromal tunnel incision allows a self-sealing injection. C) Scanning electron micrograph of polystyrene ferromagnetic beads. Scale bar: 10μm. D) Soft iron head tip for precise redistribution of beads. E) Magnetic manipulation allows beads to be drawn into the iridocorneal angle. The disruption of aqueous outflow is reduced with maintenance of a clear visual axis. Arrows show injection tract. F) Example IOP profiles of two animals following injection of magnetic microspheres into the left eye; pressure increase is either moderate (top) or acute (bottom) and sustained for 3-4 weeks with a single injection. Error bars show SD.

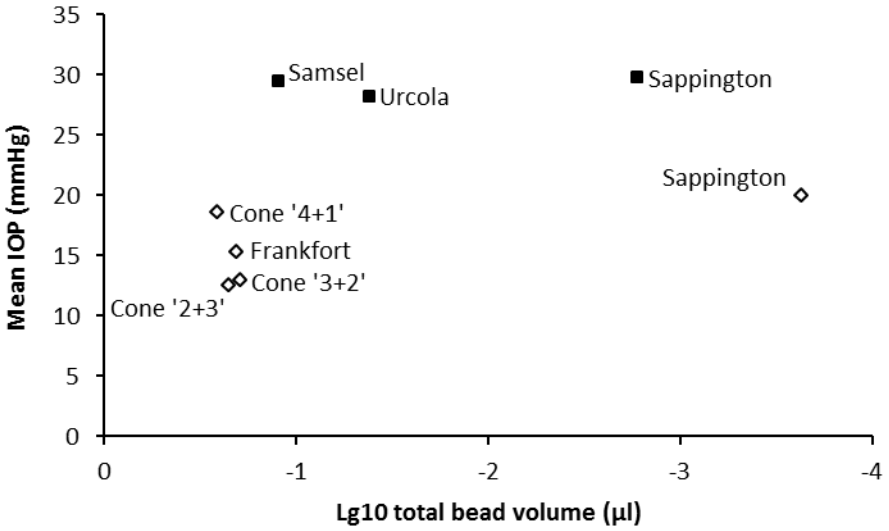

Figure2. The injected volume of beads (i.e. without carrier) has little impact on the mean IOP achieved in the Mouse (white) and Rat (black). The volume of beads delivered varies among methods by up to 3 orders of magnitude.

References

Asrani S, Zeimer R, Wilensky J, Gieser D, Vitale S, Lindenmuth K. Large Diurnal Fluctuations in Intraocular Pressure Are an Independent Risk Factor in Patients With Glaucoma. Journal of Glaucoma. 2000 Apr 1;9(2):134.

Baltan S, Inman DM, Danilov CA, Morrison RS, Calkins DJ, Horner PJ. Metabolic Vulnerability Disposes Retinal Ganglion Cell Axons to Dysfunction in a Model of Glaucomatous Degeneration. Journal of Neuroscience. 2010 Apr 21;30(16):5644–52.

Bawa G, Tkatchenko TV, Avrutsky I, Tkatchenko AV. Variational analysis of the mouse and rat eye optical parameters. Biomed Opt Express. 2013;4(11):2585–95.

Bunker S, Holeniewska J, Vijay S, Dahlmann-Noor A, Khaw P, Ng Y-S, et al. Experimental Glaucoma Induced by Ocular Injection of Magnetic Microspheres. J Vis Exp. 2015 Feb 2;(96):e52400–0.

Burgoyne CF, Downs JC, Bellezza AJ, Suh J-KF, Hart RT. The optic nerve head as a biomechanical structure: a new paradigm for understanding the role of IOP-related stress and strain in the pathophysiology of glaucomatous optic nerve head damage. Progress in retinal and eye research. 2005 Jan;24(1):39–73.

Cone FE, Steinhart MR, Oglesby EN, Kalesnykas G, Pease ME, Quigley HA. The effects of anesthesia, mouse strain and age on intraocular pressure and an improved murine model of experimental glaucoma. Experimental Eye Research. 2012 Jun;99:27–35.

Dai C, Khaw PT, Yin ZQ, Li D, Raisman G, Li Y. Structural basis of glaucoma: The fortified astrocytes of the optic nerve head are the target of raised intraocular pressure. Glia. Wiley Subscription Services, Inc., A Wiley Company; 2012 Jan 1;60(1):13–28.

Fine IH. Architecture and construction of a self-sealing incision for cataract surgery. Journal of Cataract & Refractive Surgery. 1991 Jan;17:672–6.

Foxton RH, Finkelstein A, Vijay S, Dahlmann-Noor A, Khaw PT, Morgan JE, et al. VEGF-A Is Necessary and Sufficient for Retinal Neuroprotection in Models of Experimental Glaucoma. Am J Pathol. 2013 Apr;182(4):1379–90.

Frankfort BJ, Khan AK, Tse DY, Chung I, Pang J-J, Yang Z, et al. Elevated intraocular pressure causes inner retinal dysfunction before cell loss in a mouse model of experimental glaucoma. Invest Ophthalmol Vis Sci. Association for Research in Vision and Ophthalmology; 2013 Jan;54(1):762–70.

Gaasterland D, Kupfer C. Experimental glaucoma in the rhesus monkey. Invest Ophthalmol. 1974 Jun;13(6):455–7.

Gherezghiher T, March WF, Nordquist RE, Koss MC. Laser-induced glaucoma in rabbits. Experimental Eye Research. 1986 Dec;43(6):885–94.

John S. Mechanistic insights into glaucoma provided by experimental genetics the cogan lecture. Invest Ophthalmol Vis Sci. 2005.

John S, Smith R, Savinova O. Essential iris atrophy, pigment dispersion, and glaucoma in DBA/2J mice. … and Visual Science. 1998.

Johnson EC, Doser TA, Cepurna WO, Dyck JA, Jia L, Guo Y, et al. Cell proliferation and interleukin-6-type cytokine signaling are implicated by gene expression responses in early optic nerve head injury in rat glaucoma. Invest Ophthalmol Vis Sci. 2011 Jan;52(1):504–18.

King W, Sarup V, SauveY, Moreland C, Carpenter D, Sharma S. Expansion of visual receptive fields in experimental glaucoma. Visual neuroscience. 2006;23(01):137–42.

Matsumoto Y, Johnson DH. Trabecular meshwork phagocytosis in glaucomatous eyes. Ophthalmologica. 1997;211(3):147–52.

Ma Y, Bin Shen, Zhang X, Lu Y, Chen W, Ma J, et al. Heritable Multiplex Genetic Engineering in Rats Using CRISPR/Cas9. Xu X, editor. PloS one. 2014;9(3):e89413.

Morrison JC, Johnson E, Cepurna WO. Rat models for glaucoma research. Progress in Brain Research. Elsevier; 2008. pp. 285–301.

Quigley HA, Addicks EM. Chronic experimental glaucoma in primates. I. Production of elevated intraocular pressure by anterior chamber injection of autologous ghost red blood cells. Invest Ophthalmol Vis Sci. 1980 Feb;19(2):126–36.

Quigley HA. Neuronal death in glaucoma. Progress in retinal and eye research. 1999 Jan;18(1):39–57.

Ruixia Li JHKL. Telemetric monitoring of 24 h intraocular pressure in conscious and freely moving C57BL/6J and CBA/CaJ mice. Molecular Vision. Emory University; 2008;14(11):745–9.

Remtulla S, Hallett PE. A schematic eye for the mouse, and comparisons with the rat. Vision Research. 1985 Jan;25(1):21–31.

Samsel PA, Kisiswa L, Erichsen JT, Cross SD, Morgan JE. A novel method for the induction of experimental glaucoma using magnetic microspheres. Invest Ophthalmol Vis Sci. Association for Research in Vision and Ophthalmology; 2011 Mar;52(3):1671–5.

Sander JD, Joung JK. CRISPR-Cas systems for editing, regulating and targeting genomes. Nature biotechnology. Nature Publishing Group; 2014 Apr 1;32(4):347–55.

Smedowski A, Pietrucha-Dutczak M, Kaarniranta K, Lewin-Kowalik J. A rat experimental model of glaucoma incorporating rapid-onset elevation of intraocular pressure. Scientific Reports. Nature Publishing Group; 2014 Aug 1;4.

Urcola JH, Hernández M, Vecino E. Three experimental glaucoma models in rats: comparison of the effects of intraocular pressure elevation on retinal ganglion cell size and death. Experimental Eye Research. 2006 Aug;83(2):429–37.

Vecino E, Sharma SC. Glaucoma Animal Models, Glaucoma -Basic and Clinical Concepts, InTech, 2011; pp. 319-334

Wang W-H, Millar JC, Pang I-H, Wax MB, Clark AF. Noninvasive measurement of rodent intraocular pressure with a rebound tonometer. Invest Ophthalmol Vis Sci. Association for Research in Vision and Ophthalmology; 2005 Dec;46(12):4617–21.

Weber AJ, Zelenak D. Experimental glaucoma in the primate induced by latex microspheres. Journal of neuroscience methods. 2001;111(1):39–48.

Zhang D, Vetrivel L, Verkman AS. Aquaporin deletion in mice reduces intraocular pressure and aqueous fluid production. J Gen Physiol. Rockefeller Univ Press; 2002 Jun;119(6):561–9.